MODELLING REFLECTIONS IN MILLIMETER-WAVE COMMUNICATIONS

A Project Report

submitted by

AROON NARAYANAN

in partial fulfilment of requirements
for the award of the dual degree of

BACHELOR OF TECHNOLOGY AND MASTER OF TECHNOLOGY

DEPARTMENT OF ELECTRICAL ENGINEERING
INDIAN INSTITUTE OF TECHNOLOGY MADRAS

JUNE 2017

THESIS CERTIFICATE

This is to certify that the thesis titled **MODELLING REFLECTIONS IN MILLIMETER WAVE COMMUNICATIONS**, submitted by **Aroon Narayanan**, to the Indian Institute of Technology, Madras, for the award of the degrees of **Bachelor of Technology and Master of Technology**, is a bona fide record of the research work done by him under our supervision. The contents of this thesis, in full or in parts, have not been submitted to any other Institute or University for the award of any degree or diploma.

Dr. Radha Krishna Ganti
Research Guide
Associate Professor
Dept. of Electrical Engineering
IIT-Madras, 600 036

Place: Chennai

Date: 9th June 2017

ACKNOWLEDGEMENTS

I am indebted to Dr. Radha Krishna Ganti for his valuable guidance and motivation throughout this project. Thanks to him, this project has been a unique learning opportunity for me.

My sincere gratitude also to Dr. Sreejith T V, who mentored me throughout the project and provided important academic counselling at crucial junctures. His intellectual contributions to this project are many and significant.

I am also thankful for my parents, teachers, and friends, all of whom provided important support of varying kinds that helped me finish this project.

ABSTRACT

KEYWORDS: Reflections; mmwave; Stochastic Geometry; Coverage.

The coverage probability of a user in a mmwave system depends on the availability of line-of-sight paths or reflected paths from any base station. Many prior works modelled blockages using random shape theory and analyzed the SIR distribution with and without interference. While it is intuitive that the reflected paths do not significantly contribute to the coverage (because of longer path lengths), there are no works which provide a model and study the coverage with reflections. In this project, the impact of reflectors using stochastic geometry is modelled and analyzed. It is observed that the reflectors have very little impact on the coverage probability.

TABLE OF CONTENTS

LIST OF TABLES

LIST OF FIGURES

ABBREVIATIONS

mmWave	Millimeter Wave
5G	Fifth-Generation
LOS/NLOS	Line Of Sight/Non Line Of Sight
SINR	Signal to Interference plus Noise Ratio
PPP	Poisson Point Process
AWGN	Additive White Gaussian Noise
BS	Base Station
UE	User Equipment
CCDF	Complementary Cumulative Distribution Function

NOTATION

α	Path loss
λ	PPP density
r	Distance from origin
l	Dimension (length) of objects
θ	Orientation of objects
σ	Standard Distribution of noise

CHAPTER 1

INTRODUCTION

Current cellular systems predominantly operate in the 1-6 GHz range of spectrum. In these frequencies, radio signals can propagate around an object, and it supports radio communication when a mobile device is blocked or shadowed by an obstruction. The next generation of wireless standards are looking at higher operating frequencies, mainly due to spectrum availability. Millimeter wave (mmWave) spectrum is the range of frequencies from 28-90 GHz, and is being envisioned to augment the existing frequencies in the 5G standard Pi and Khan (2011). Measurements have reaffirmed the feasibility of mmWave in the urban environment Rappaport *et al.* (2013*b*) and measurements for indoor communication at mmWave frequencies show that it holds promise with indoor stations MacCartney *et al.* (2016). Diffraction is a powerful propagation mechanism in today's 3G and 4G cellular systems but becomes very lossy at mmWave frequencies due to the small wavelengths of these bands. However, scattering and reflection become dominant at mmWave frequencies Pi and Khan (2011). Also, mmWave communication has been shown to be more sensitive to propagation loss than current modes of communication Alejos *et al.* (2008).

As has been shown in earlier works Xu *et al.* (2002); Ben-Dor *et al.* (2011), first order reflections, i.e., paths from one point to another using one reflector, and second order reflections, i.e., paths from one point to another using two reflector, are important features at millimeter wave frequencies, especially by metallic objects. A later work Rajagopal *et al.* (2012) finds that well-known lossy objects such as human body and concrete are good reflectors at mmWave frequencies, enabling the receiver to capture secondary reflections for non-line-of-sight communication. Many other common objects have been shown in these works as having high reflection coefficients, which makes them a useful component of signal processing. Measurements for mmWave have revealed that the path loss characteristics for LOS and NLOS links are considerably different Rappaport *et al.* (2013*b*) Rappaport *et al.* (2013*a*) Rajagopal *et al.* (2012).

The coverage of mmwave systems with blockages is analyzed in Akdeniz *et al.* (2014) using statistical models and in Bai *et al.* (2012) Bai *et al.* (2014) using tools from

stochastic geometry. However, in these works, reflectors are not considered and only blockages are taken into account. However, as shown in Xu *et al.* (2002), reflections can contribute to the signal power, particularly if the LOS path is blocked. A later work Akoum *et al.* (2012) incorporated NLOS communication as well, but this model did not incorporate tractable randomly-placed reflectors.

In this project, we look at the coverage in a mmwave system with both blockages and reflectors. Similar to the blockage model, we introduce a stochastic model for reflectors and analyse the coverage (SINR distribution).

CHAPTER 2

SYSTEM MODEL

We consider a wireless network on the 2-D plane in the presence of both line-of-sight signal blockages and reflectors. Our main motivation is to characterise the effects of reflectors on the coverage probability of a typical user.

2.1 Base Stations

The locations of the mmwave base stations are modelled by a spatial Poisson Point Process (PPP), $\Phi \subset \mathbb{R}^2$, with density λ. A standard path loss model $l(x) = \|x\|^{-\alpha}$, $\alpha > 2$, is assumed. For any pair of nodes x and y, independent Rayleigh fading (power) with unit mean is assumed and is denoted by h_{xy}. The noise term is assumed to be circularly symmetric complex Gaussian noise (AWGN) with zero mean and variance σ^2.

2.2 Blockages and Reflectors

Random shape theory is used in this paper to populate the environment with objects. There are two types of objects - blockages and reflectors - and both of these are taken as 2D straight line segments with random length and orientation that we describe later. Blockages are objects that are obstruction to any path, LOS or NLOS, between a base station and a user, but these do not reflect signals *i.e.*, their reflection coefficient is zero. Reflectors are objects that can reflect the signals *i.e.*, their reflection coefficient is non-zero. All objects in this model, both blockages and reflectors, have zero transmission coefficient, which means that all of them will attenuate to zero any signal that attempts to *pass through them*. This model of blockages has been used in Bai *et al.* (2012).

The centres of the objects form a spatial PPP Φ_o of density λ_o of which a fraction δ are able to reflect the signals, *i.e.*, the density of reflecting objects, $\lambda_R = \delta\lambda_o$ and that of

blockages is $\lambda_R = (1-\delta)\lambda_o$. Hence the centres of the reflectors form a spatial PPP Φ_R of density λ_R which is a thinned version of Φ_o and the centres of the blockages form a spatial PPP Φ_B of density λ_B. Both the reflectors and blockages are assumed to be lines segments with random length l and orientated at angle θ with the radial line from user to centres of the objects as shown in Fig.3.1. The dimension l is uniformly distributed in $[L_1, L_2]$, and the orientation of line segments θ is uniformly distributed in $[0, 2\pi)$.

2.3 Association Strategy

A user can connect to a BS either by a direct path or a reflected path. We assume the user always connected to the BS which is having the shortest distance either through the direct path which is visible or through indirect path provided by the reflectors. Hence, the received signal-to-interference plus noise ratio (SINR) is given by,

$$\mathbf{1}(r_d < r_r)\frac{P_t|h_d|^2 r_d^{-\alpha}}{\sigma^2 + I_D + I_R} + \mathbf{1}(r_r < r_d)\frac{P_t|h_r|^2 r_r^{-\alpha}}{\sigma^2 + I_D + I_R}, \tag{2.1}$$

where r_d is the distance to the nearest visible BS and r_r is the length of the shortest reflected path from any BS through a reflector. Here $\mathbf{1}(.)$ is the indicator function and h_d and h_r are the fading coefficients. I_R and I_D are the interference due to the reflected paths and the direct paths, respectively. α is the path loss coefficient. In this project, we are studying a simple model where the environment that these signals pass through are uniform. As a result, α for both the direct path and the reflected path will be the same. Moreover, the reflection coefficient is taken to be one, so there's no energy loss due to the reflection at the reflector. We have only considered first-order reflections, but it should be noted that in the practical case, there will be many other effects adding to NLOS coverage, including multi-step reflections and diffraction. Hence, there can be a difference in α for LOS and NLOS path loss coefficients in the real scenario, as measured in Rappaport *et al.* (2013*b*).

CHAPTER 3

ANALYSIS

3.1 Distance Distributions

In this section, we will describe the distribution of r_r and r_d distances which characterize the SINR.

3.1.1 Distribution of shortest direct path

When the BS density is λ and that of blockages is λ_B, the distribution of distance to the closest visible base station, r_d, is derived in Bai *et al.* (2012) and is given by,

$$f_{R_d}(r_d) = 2\pi\lambda r_d \exp(-\lambda\pi r_d^2 S(r_d) - \beta r_d),$$

where $\beta = 2(\lambda_B + \lambda_R)L_b/\pi = 2\lambda_o L_b/\pi$. Here $L_b = \mathbb{E}[l]$ is the expected length of the blockage and $S(x) = \frac{2}{\beta^2 x^2}(1-e^{-x\beta}(1+\beta x))$. They have also shown that the probability of blockage depends on the length of the path. For a BS x, the probability that its path to the origin is blocked is given by

$$P_b(x) = \exp(-\beta\|x\|). \tag{3.1}$$

3.1.2 Distribution of distance to nearest visible reflector

We assume that a reflector is blocked if its centre is not visible from the origin (location of a typical UE). This is a reasonable assumption if the density of the reflectors and the length of the reflectors is small. Since the reflectors are distributed according to PPP of density λ_R and blockage density λ_B, the distance to the centre of the closest visible reflector, d, is distributed according to:

$$f_D(d) = 2\pi\lambda_R d \exp(-\lambda_R\pi d^2 S(d) - \beta d).$$

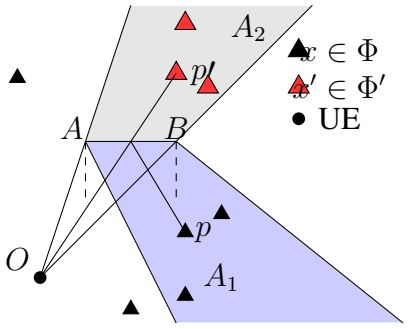

Figure 3.1: Illustration of deformed PPP. Here, AB is the reflector which reflects the signal from BS p to the user located at O. Original PPP (black triangles) is Φ and the deformed PPP (red triangle) about AB is denoted by Φ'. The reflected point in the transformed PPP is shown as p'.

3.1.3 Distribution of shortest reflected path

In Fig. 3.1, AB represents a mirror and O represents the UE receiver at the origin. We first observe that only the BS in the shaded region $A_1 \subset \mathbb{R}^2$ can reflect of AB and reach the origin. Signals from BSs in $\mathbb{R}^2 \setminus A_1$ cannot reach the origin through the reflector AB. The total length that a signal propagates for a reflected path equals the distance to the mirror and the distance from the mirror to the user at the origin. In order to characterise the distribution of the shortest reflected path, we project each of the possible base stations as shown in Fig. 3.1. The region A_2 denotes the mirror image of the region A_1 and for computing the length of the reflected path, a BS $y \in A_1$ can be mirror imaged to $y\prime \in A_2$. The number of reflected base stations in the semi-conic region on the other side will be always equal to the number of base stations on the original side due to symmetry, so the density of base stations of the transformed PPP in the reflected semi-conic region will be λ_B in the region A_2. These reflected points may or may not be visible to the user, depending on whether there are blockages on the link between the points and the user. We now characterise the length of the shortest reflected path for a reflector at a distance d.

Lemma 1. *Given λ, λ_B and λ_R are the densities of BSs, blockages and reflectors respectively, the conditional CDF of the distance of shorted reflected path, r_r, when the nearest reflector is at a distance d is given by,*

$$\mathbb{P}(R_f > r_r | d, \theta) = \mathbb{E}_l \exp\left(- \int_{\mathcal{A}(\theta,d)} \lambda e^{-\beta ||x||} \mathrm{d}x \right),$$

where $\mathcal{A}(\theta, d) = B(0, r_r) \cap A_2(\theta, d)$. Here θ represents the orientation of the reflector.

Proof. Suppose that the user is located at the origin, O and the nearest reflector is at a distance d from it as shown in Fig.3.2. Let the shortest visible reflecting BS after the transformation of ϕ, $p' \in \phi'$, is at a distance x from the user at origin. Remember x is the total distance of the reflected path in the original PPP. Note that the distance to the nearest visible BS p' is larger than x if and only if all the base stations located within the shaded region $\mathcal{A}(\theta, d)$ are not visible to the user. Let $V_{x|d}$ denote the event that x is visible given d. We have

$$\begin{aligned}\mathbb{P}(R_f > r_r|d) &= \mathbb{E}\left[\prod_{x\in\mathcal{A}(\theta,d)\cap\Phi}\left(1-\mathbf{1}(V_{x|d})\right)\right], \\ &\overset{(a)}{=} \mathbb{E}\left[\prod_{x\subset\mathcal{A}(\theta,d)\cap\Phi}(1-e^{-\beta||x||})\right], \\ &\overset{(b)}{=} \mathbb{E}_l \exp\left(-\int_{\mathcal{A}(\theta,d)}\lambda e^{-\beta||x||}\mathrm{d}\mathbf{x}\right),\end{aligned}$$

where (a) follows from (3.1) and (b) follows from the PGFL property of a PPP. □

Observe that $\mathcal{A}(\theta, d) = B(0, r_r) \cap A_2(\theta, d)$ is a complicated region for integration. To simplify the integral further, we make the following assumption: *We assume that the reflectors are perpendicular to the line connecting the UE and the reflector's center,* i.e., $\theta = \pi/2$.

The distribution of the shortest reflecting path length is given in the following corollary.

Corollary 1. *Given λ, λ_B and λ_R are the densities of BSs, blockages and reflectors respectively, the conditional distribution of the distance of shorted reflected path, r_r, when the nearest reflector is at a distance d is given by,*

$$f_{R_f}(r_r|d) \approx \mathbb{E}_l\left[\lambda\theta_d K^{'}(r_r)e^{-\lambda\theta_d K(r_r)}\right],$$

where $\theta_d = \arctan(l/2d)$ and $K(r_r)$ is given by

$$K(r_r) = 2\left[\frac{e^{-\beta d}}{\beta}(d+\frac{1}{\beta}) - \frac{e^{-\beta r_r}}{\beta}(r_r+\frac{1}{\beta})\right]$$

and $K^{'}(r_r) = 2\left(e^{-\beta r_r}\left(\frac{1}{\beta}+r_r\right) - \frac{e^{-\beta r_r}}{\beta}\right)$ is the first derivative of $K(r_r)$. Here $\mathbb{E}_l$ is

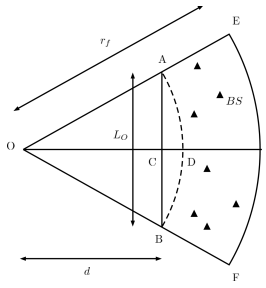

Figure 3.2: Illustration of approximation of shortest reflection path distribution. AB is the reflector of length l and at a distance $OC = d$ from the user at O. Also AB is assumed perpendicular to the radial line from user to reflector centre. The region $\mathcal{A}$ over which integration is done is approximated to the region between the two arcs, labelled $ABFE$. The nearest reflected BS is p' which is at a distance r_r.

the expectation with respect to length of the reflector.

Proof.

$$\begin{aligned}\mathbb{P}(R_f > r_r|d) &= \exp\left(-\int_{\mathcal{A}} \lambda e^{-\beta||x||}\mathrm{d}\mathbf{x}\right)\\ &\overset{(a)}{\approx} \exp\left(-\int_{\theta=-\theta_d}^{\theta_d}\int_{r=d}^{r_r} \lambda e^{-\beta r} r\mathrm{d}r\mathrm{d}\theta\right)\\ &= \exp(-\lambda\theta_d K(r_r)).\end{aligned}$$

Here in (a), area of shaded region $\mathcal{A} \approx \theta_d(r_r^2 - d^2)$ by approximating the reflector perpendicular to d as an arc of length l which subtend $\angle COB = \theta_d$. Then by finding negative derivative, $-\frac{\mathrm{d}}{\mathrm{d}r}\mathbb{P}(R_f > r_r|d)$ gives the PDF. □

Assuming that that the shortest reflected path is through the closest visible reflector, the distribution of r_r can be obtained by unconditioning the conditional density function using the following property of conditional and joint distributions functions, $f(x, y) = f(x|y)f(y)$. Consider the CCDFs of the direct path length and reflected path length, it can be easily verified that

$$\mathbb{P}[R_d = \infty] = e^{-\frac{2\pi\lambda}{\beta^2}},$$

which implies that there is a finite probability that there is no direct path to the typical user at the origin. This might happen when all the BSs to the user at the origin are

blocked. Similarly,

$$\mathbb{P}[R_r = \infty | d] = \mathbb{E}_l e^{-\int_{\mathcal{A}_2(\theta,d)} \lambda e^{-\beta||x||} \mathrm{d}\mathbf{x}}$$
$$\approx \mathbb{E}_l \left[\exp(-2\lambda\theta_d e^{-\beta d}(d/\beta + 1/\beta^2)) \right],$$

which is finite and non-zero for all combinations of λ, λ_o. This implies that there is no reflected path. This result is different from the the conventional cellular case, $\mathbb{P}[R > r] = e^{-\lambda r^2}$ which tends to zero as $r \to \infty$. The presence of blockages not just increases the shortest connected path but can also make a user to be uncovered by the network. Mean distances are plotted in Figure 3.3. From Figure 3.3, we can see that both the direct distance and the reflected distances are decreasing with increasing BS density. We can also see that when the dimension of reflectors increases, the shortest reflected path distance decreases. That makes sense as as it is more likely for a user to get more reflections with increasing length of reflectors.

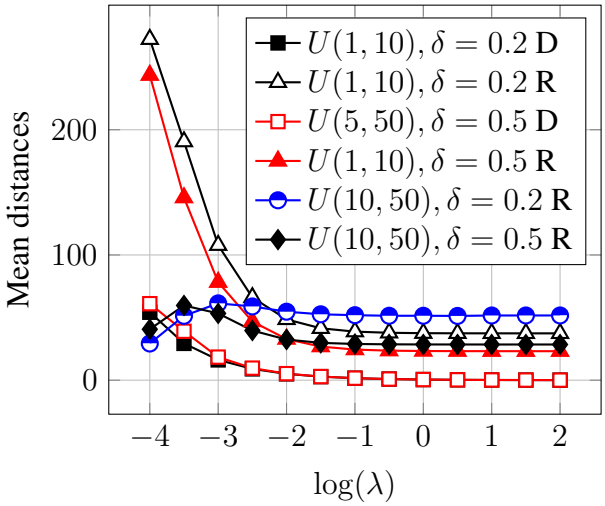

Figure 3.3: Mean of shortest direct path and reflected path lengths Vs BS density for $\lambda_B = 10^{-3}$, $\lambda_R = 10^{-3}$, *i.e.*, $\lambda_o = 2 \times 10^{-3}$ with different δ and different dimensions for objects. The dimension of objects are distributed uniformly, $l \sim U(L_1, L_2)$.

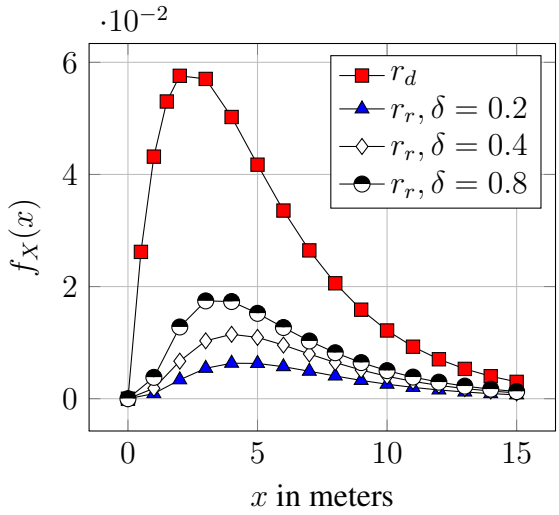

Figure 3.4: Distance distributions of r_r and r_d for different reflection densities with $\lambda = 10^{-2}, \lambda_o = 10^{-1}$.

3.1.4 Association Probabilities

Since the association is assumed to be nearest connectivity either through direct visible path or a reflected path, the probability of direct connectivity for a typical user is,

$$p_d = \mathbb{P}(r_d > r_r) = \int_0^\infty \int_{r_r}^\infty f_{R_f}(r_r) f_{R_d}(r_d) \mathrm{d}r_d \mathrm{d}r_r \tag{3.2}$$

Similarly, the probability of reflected connectivity is,

$$p_r = \mathbb{P}(r_d < r_r) = \int_0^\infty \int_{r_d}^\infty f_{R_f}(r_r) f_{R_d}(r_d) \mathrm{d}r_r \mathrm{d}r_d \tag{3.3}$$

3.2 Coverage Probability

Coverage probability for a user is defined as the probability that the signal received by the user has an SINR greater than a threshold, T to establish the connectivity. In theorem.1 we will provide the coverage probability for a typical user.

Theorem 1. *The coverage probability $\mathbb{P}_C(T)$ for a user connected to base stations either through the direct path or the reflected path is*

$$\mathbb{P}_C(T) = P_D(T) + P_R(T), \tag{3.4}$$

where $P_D(T)$ is the coverage probability of a user connected through the direct path,

given by,

$$P_D(T) = \mathbb{E}_{r_d<r_r}\Bigg[e^{-2\pi\lambda\int_{r_d}^{\infty}\left(\frac{Tr_d^{\alpha}r^{-\alpha}e^{-\beta r}}{1+Tr_d^{\alpha}r^{-\alpha}}\right)r\mathrm{d}r} \times \left(1-\frac{Tr_d^{\alpha}r_r^{-\alpha}e^{-\beta r_r}}{1+Tr_d^{\alpha}r_r^{-\alpha}}\right)e^{-r_d^{\alpha}\sigma^2T}\Bigg].$$

$P_R(T)$ *is the coverage probability of a user connected through the reflected path, given by,*

$$P_R(T) = \mathbb{E}_{r_d>r_r}\Bigg[e^{-2\pi\lambda\int_{r_r}^{\infty}\left(\frac{Tr_r^{\alpha}r^{-\alpha}e^{-\beta r}}{1+Tr_r^{\alpha}r^{-\alpha}}\right)r\mathrm{d}r}e^{-r_r^{\alpha}\sigma^2T}\Bigg].$$

Proof. See Appendix. □

CHAPTER 4

RESULTS AND CONCLUSIONS

4.1 Results

In this Section, we numerically evaluate the coverage probability given in Theorem 1 and compare with our theoretical derivations. We simulated a square area in which base stations, blockages and reflectors are distributed according to PPPs such that there are at least 100 base stations on average in the area and $\alpha = 4$. The objects (blockages and reflectors) had lengths chosen from a uniform distribution, $U(L_1, L_2)$ and the orientation of reflectors and blockages are uniformly distributed *i.e.*, $\theta \sim U(0, 2\pi)$. It must be noted that our approximations in our analysis is valid only for cases in which the length of objects is comparable to, or smaller than, the mean distance between objects, *i.e.*, $\min(\frac{1}{2\sqrt{\lambda_O}}, \frac{1}{2\sqrt{\lambda}})$. This is because in analysis we approximated reflector as an arc, however this makes the objects not overlapping as in the practical scenario.

The average lengths of shortest visible direct path and the reflected path through nearest visible reflector are given in Table 4.1. We observe that as the reflector density is increased, the reflected path length shortens as there are more reflectors. The shortest direct path length is not varying as the density of blockages remain the same. We also observe that undercertain configurations, the average length of the reflected path is very similar to the length of the direct path.

Table 4.1: Mean distances of shortest direct path and reflected path for different fractions of reflectors. r_c denotes the connected BS distance in no blockage and no reflectors case.

(λ, λ_o)	l	r_c	r_d		r_r	
			$\delta = 0.2$	0.5	0.2	0.5
$(10^{-1}, 10^{-1})$	(1,5)	1.58	1.84	1.84	6.03	5.94
$(10^{-1}, 10^{-2})$	(1,5)	1.58	1.61	1.61	16.23	10.70
$(10^{-2}, 10^{-2})$	(1,10)	5	5.42	5.42	29.49	23.69
$(10^{-3}, 10^{-3})$	(1,10)	15.81	16.19	16.19	151.94	112.29

From the simulations and theory, the probability of the user connecting to the direct path is very high for most cases, so mostly the user will be tagged to nearest visible BS instead of getting connected through a reflected path. These probabilities are plotted in Figure 4.1.

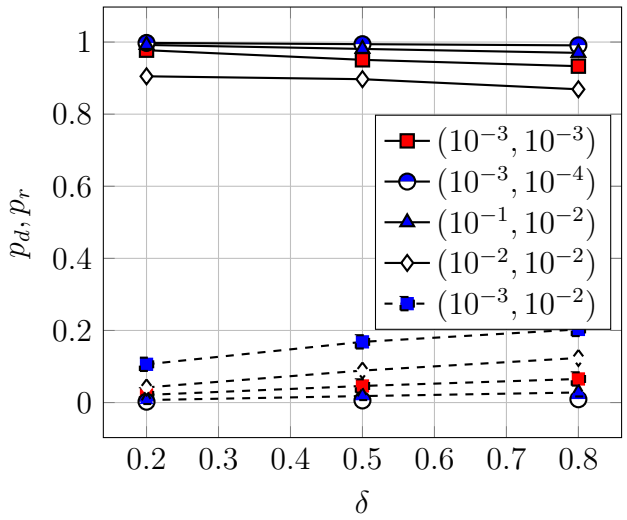

Figure 4.1: Probability of connecting through shortest direct path and shortest reflected path Vs different relative reflector density factor, δ. The BS density and objects densities are given in as (λ, λ_o), length of objects $l \sim U(L_1, L_2)$m, solid lines represent the direct connection and dashed lines for reflected connection.

As expected, the probability of the user connecting to the reflected path increases in urban environments with a high density of reflecting objects, such as metallic objects, as compared to the density of base stations. This can be seen from $(10^{-3}, 10^{-2}), \delta = 0.2$ and $(10^{-3}, 10^{-2}), \delta = 0.5$. This implies that a measurable gain in coverage is possible by reflectors. This is can be verified from coverage probability Fig.4.3. Also, our theory does not consider reflections from the reflectors other than the closest one. When the density of reflector is high, it is likely that the user can connect to a BS through a shortest reflected path from reflector other than the closest reflector as well.

In Figures 4.2 and 4.3, the coverage probability is plotted for various scenarios. We first observe that the MonteCarlo simulations match the results. We also observe that the improvement in coverage is very minor because of the reflectors. For reference, we have also plotted the coverage probability of a networks without any blockages and reflectors.

When the number of objects is increased while keeping the number of base stations fixed, there are multiple effects to be considered. There will be a higher probability

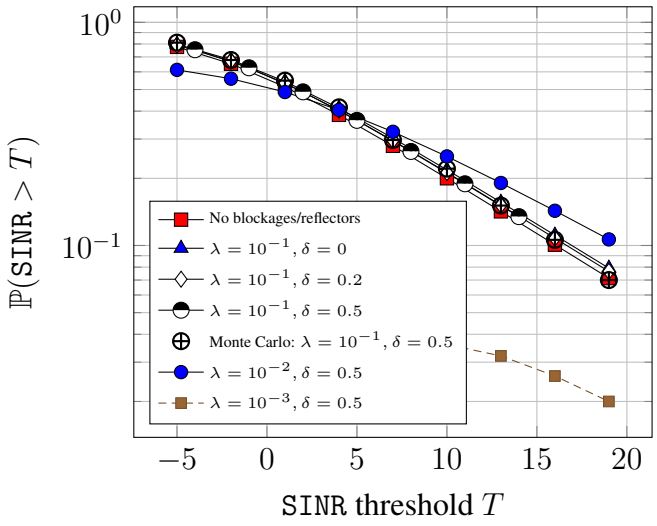

Figure 4.2: Comparison of coverage probabilities for cellular case without blockages and reflections and with blockages only and with both blockages and reflections. The BS density $\lambda = 10^{-1}$, total object density $\lambda_o = 10^{-2}$ of which δ percentage of objects are reflecting. The length of objects are assumed to be uniformly distributed in all cases.

of blockage due to higher number of objects, and added reflectors can contribute useful signal as well as interference. It is a well established result that the coverage probability of cellular network in interference limited scenario is independent of the BS density. It can be seen that the presence of objects changes the coverage probability with density of BS. For high dense network with moderate density of blockages and reflectors improve the coverage probability, intuitively we can say that blockages reduces the interfering signals. For low density networks, presence of high density of reflectors and blockages reduces the coverage probability drastically as most of the links are blocked by the objects. For dense networks when the blockages and reflectors are introduced, the coverage probability improves, because of the eliminating a large portion of interference at the same time direct strong interference can also be blocked and when the fraction of reflecting objects are increased the effect of interference through the reflected path increases which causes the coverage to be reduced. In this study we have considered only primary reflections and in analysis we have incorporated only the reflection caused by the nearest visible BSs. It can be observed that strong reflections can also be caused by other nearby reflectors also, which can also cause the coverage to be varied.

The reflected signal almost covers double the distance of that of direct path most of the cases and hence for the cases with low density of reflectors, the reflectors will not affect the coverage probability, but when the density of the reflector is comparable or

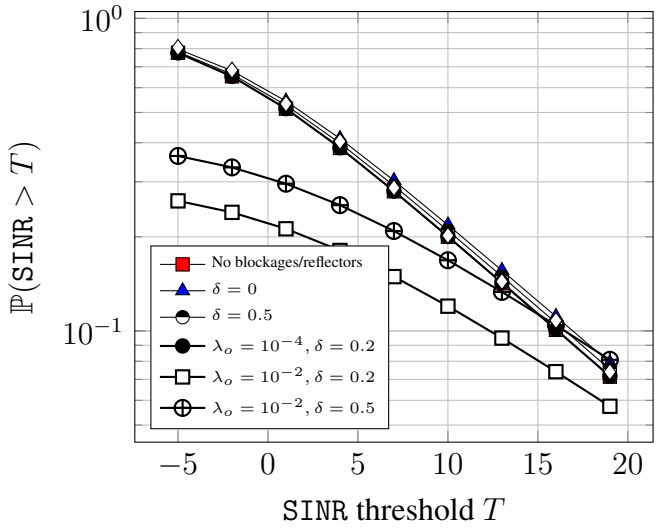

Figure 4.3: Comparison of coverage probabilities for cellular case without blockages and reflections and with blockages only and with both blockages and reflections. The BS density $\lambda = 10^{-3}$, total object density $\lambda_o = 10^{-3}$ of which δ percentage of objects are reflecting. The length of objects are assumed to be uniformly distributed in all cases. *i.e.*, $l \sim U(1, 10)$m.

more than BS density, interference starts to dominate. This can be seen for the case of $\delta = 0.5$.

Table 4.2: Mean and and probabilities of shortest direct path and nearest visible reflector

$(\lambda, \lambda_B, \lambda_R)$	r_d	r_{r1}
Mean	17.1	57.4
Probability	0.983	0.017

4.2 Conclusion

In this project, we have proposed a method to model and analyse the reflections in a mmwave cellular system. We have analysed the coverage probability for cellular networks considering the effects of reflections and blockages. It is found that the coverage probability is sensitive to the presence of objects. It is noticed that presence of high density of reflectors can improve the coverage in high density networks and in low density networks the reflected signals has to travel longer distances than that of direct path and coverage probability has no further changes from that of blockages. Also it should be mentioned that in this analysis the reflectors are placed randomly and we believe that proper design and placement of reflectors can improve the performance of the network.

CHAPTER 5

LIMITATIONS

Due to the complexity of modeling reflections, some assumptions had to be made in order to simplify the analysis. These are presented here and justified.

5.1 Reflection Through Closest Reflector Only

5.1.1 Assumption

Ideally, the user should connect to the base station with the shortest total reflected distance, regardless of which reflector this happens through. We have assumed that the shortest reflected path is through only the reflector closest to the user.

5.1.2 Reason

The distribution of the shortest total reflected distance has been found by conditioning on the distance from the user to the reflector through which the reflection is happening (refer Lemma 1).

The easiest way of characterizing the distance from the user to the reflector through which the reflection is happening is to take this reflector as the closest reflector.

5.1.3 Validity

As seen from the results, the reflected path is through the closest reflector in only 20 percent of the cases on average.

5.2 Orientation Of Reflector Is Perpendicular

5.2.1 Assumption

As can be seen in Fig 1, the reflector can be randomly oriented. However, we have taken the reflector as perpendicular the line connecting the user to the reflector's center.

5.2.2 Reason

In the derivation of Corollary 1, this assumption makes the integration easier.

APPENDIX A

DERIVING COVERAGE PROBABILITY

The user in this model connects to both the reflected path and direct path, if they exist. Given the nearest direct BS is at a distance, r_d from the user and the nearest reflecting BS is at a distance r_r, we have

$$\mathbb{P}[\mathtt{SINR} > T] = \mathbb{E}_{r_d, r_r}\Big[\mathbb{P}[\mathtt{SINR}_D > T | r_d < r_r] + \mathbb{P}[\mathtt{SINR}_R > T | r_d > r_r]\Big],$$

where $\mathtt{SINR}_D = \frac{|h|^2 r_d^{-\alpha}}{\sigma^2 + \mathbf{I}_D}$ is the $\mathtt{SINR}$ of user connected to visible BS and $\mathbf{I}_D$ interference seen by the direct connected UE experienced from the reflectors other than the closest reflector will be highly attenuated, we have interference for direct path,

$$\mathbf{I}_D = \sum_{\|x\| > r_d, x \in \Phi} \|x\|^{-\alpha} |h_x|^2 S_x + r_r^{-\alpha} |h_f|^2 S_{r_r}$$

Now

$$\begin{aligned}
&\mathbb{P}[\mathtt{SINR}_D > T | r_d, r_r] = \mathbb{P}\left[|h|^2 > T r_d^{\alpha}(\mathbf{I}_D + \sigma^2)\right] \\
&\overset{(a)}{=} \mathbb{E}\Big[\left(\prod_{\|x\| > r_d, x \in \Phi} e^{-T r_d^{\alpha} \|x\|^{-\alpha} |h_x|^2} e^{-\beta \|x\|}\right) + 1 - e^{-\beta \|x\|}\Big] \\
&\times \mathbb{E}_{h_f}\left(e^{-T r_d^{\alpha} r_r^{-\alpha} |h_f|^2} e^{-\beta r_r} + (1 - e^{-\beta r_r})\right) e^{-r_d^{\alpha} \sigma^2 T}, \\
&\overset{(b)}{=} \mathbb{E}\Big[\left(\prod_{\|x\| > r_d, x \in \Phi} 1 - \frac{e^{-\beta \|x\|} T r_d^{\alpha} \|x\|^{-\alpha}}{1 + T r_d^{\alpha} \|x\|^{-\alpha}}\right)\Big] \\
&\times \left(\frac{1}{1 + T r_d^{\alpha} r_r^{-\alpha}} e^{-\beta r_r} + (1 - e^{-\beta r_r})\right) e^{-r_d^{\alpha} \sigma^2 T}, \\
&\overset{(c)}{=} \exp\left(-2\pi\lambda \int_{r_d}^{\infty} \left(\frac{T r_d^{\alpha} r^{-\alpha} e^{-\beta r}}{1 + T r_d^{\alpha} r^{-\alpha}}\right) r \mathrm{d}r\right) \\
&\times \left(1 - \frac{T r_d^{\alpha} r_r^{-\alpha} e^{-\beta r_r}}{1 + T r_d^{\alpha} r_r^{-\alpha}}\right) e^{-r_d^{\alpha} \sigma^2 T}.
\end{aligned} \tag{A.1}$$

Here (a) by using the fact that $|h|^2 \sim \exp(1)$ for Rayleigh fading and (b) by using the PGFL property of PPP. Now consider the reflected $\texttt{SINR}_R$, we have,

$$\mathbf{I}_R = \sum_{\|x\|>r_d, x\in\Phi} \|x\|^{-\alpha}|h_x|^2 e^{-\beta\|x\|}$$

Similar to the above derivation,

$$\begin{aligned}
&\mathbb{P}[\texttt{SINR}_R > T | r_d, r_r] = \mathbb{P}\left[|h|^2 > T r_r^{\alpha}(\mathbf{I}_R + \sigma^2)\right] \\
&= \mathbb{E}\Big[e^{-r_r^{\alpha}\sigma^2 T} \prod_{\|x\|>r_d, x\in\Phi} \exp\left(-T r_r^{\alpha}\|x\|^{-\alpha}|h_x|^2 S_x\right)\Big] \\
&= e^{-r_r^{\alpha}\sigma^2 T} \exp\left(-2\pi\lambda \int_{r_d>r_r}^{\infty} \left(\frac{T r_r^{\alpha} r^{-\alpha} e^{-\beta r}}{1 + T r_r^{\alpha} r^{-\alpha}}\right) r \mathrm{d}r\right). \qquad \text{(A.2)}
\end{aligned}$$

APPENDIX B

PAPERS SUBMITTED

1. **Aroon Narayanan, Sreejith T. V** and **Radha Krishna Ganti** (2017). *Global Telecommunications Conference (GLOBECOM 2017)* [Submitted]

REFERENCES

1. **Akdeniz, M. R.**, **Y. Liu**, **M. K. Samimi**, **S. Sun**, **S. Rangan**, **T. S. Rappaport**, and **E. Erkip** (2014). Millimeter wave channel modeling and cellular capacity evaluation. *IEEE Journal on Selected Areas in Communications*, **32**(6), 1164–1179. ISSN 0733-8716.

2. **Akoum, S.**, **O. E. Ayach**, and **R. W. Heath**, Coverage and capacity in mmwave cellular systems. *In 2012 Conference Record of the Forty Sixth Asilomar Conference on Signals, Systems and Computers (ASILOMAR)*. 2012. ISSN 1058-6393.

3. **Alejos, A. V.**, **M. G. Sanchez**, and **I. Cuinas** (2008). Measurement and analysis of propagation mechanisms at 40 ghz: Viability of site shielding forced by obstacles. *IEEE Transactions on Vehicular Technology*, **57**(6), 3369–3380. ISSN 0018-9545.

4. **Andrews, J. G.**, **F. Baccelli**, and **R. K. Ganti** (2011). A tractable approach to coverage and rate in cellular networks. *IEEE Transactions on Communications*, **59**(11), 3122–3134. ISSN 0090-6778.

5. **Bai, T.**, **R. Vaze**, and **R. W. Heath**, Using random shape theory to model blockage in random cellular networks. *In 2012 International Conference on Signal Processing and Communications (SPCOM)*. 2012. ISSN 2165-0608.

6. **Bai, T.**, **R. Vaze**, and **R. W. Heath** (2014). Analysis of blockage effects on urban cellular networks. *IEEE Transactions on Wireless Communications*, **13**(9), 5070–5083. ISSN 1536-1276.

7. **Ben-Dor, E.**, **T. S. Rappaport**, **Y. Qiao**, and **S. J. Lauffenburger**, Millimeter-wave 60 ghz outdoor and vehicle aoa propagation measurements using a broadband channel sounder. *In 2011 IEEE Global Telecommunications Conference - GLOBECOM 2011*. 2011. ISSN 1930-529X.

8. **MacCartney, G. R.**, **S. Deng**, and **T. S. Rappaport**, Indoor office plan environment and layout-based mmwave path loss models for 28 ghz and 73 ghz. *In 2016 IEEE 83rd Vehicular Technology Conference (VTC Spring)*. 2016.

9. **Pi, Z.** and **F. Khan** (2011). An introduction to millimeter-wave mobile broadband systems. *IEEE Communications Magazine*, **49**(6), 101–107. ISSN 0163-6804.

10. **Rajagopal, S.**, **S. Abu-Surra**, and **M. Malmirchegini**, Channel feasibility for outdoor non-line-of-sight mmwave mobile communication. *In 2012 IEEE Vehicular Technology Conference (VTC Fall)*. 2012. ISSN 1090-3038.

11. **Rappaport, T. S.**, **F. Gutierrez**, **E. Ben-Dor**, **J. N. Murdock**, **Y. Qiao**, and **J. I. Tamir** (2013*a*). Broadband millimeter-wave propagation measurements and models using adaptive-beam antennas for outdoor urban cellular communications. *IEEE Transactions on Antennas and Propagation*, **61**(4), 1850–1859. ISSN 0018-926X.

12. **Rappaport, T. S.**, **S. Sun**, **R. Mayzus**, **H. Zhao**, **Y. Azar**, **K. Wang**, **G. N. Wong**, **J. K. Schulz**, **M. Samimi**, and **F. Gutierrez** (2013*b*). Millimeter wave mobile communications for 5g cellular: It will work! *IEEE Access*, **1**, 335–349. ISSN 2169-3536.

13. **Xu, H.**, **V. Kukshya**, and **T. S. Rappaport** (2002). Spatial and temporal characteristics of 60-ghz indoor channels. *IEEE Journal on Selected Areas in Communications*, **20**(3), 620–630. ISSN 0733-8716.